Title

Role of microRNA-122 in hepatic lipid metabolism of the weanling female rat offspring exposed to prenatal and postnatal caloric restriction

Authors

Dai, Yun
Ghosh, Shubhamoy
Shin, Bo-Chul
et al.

Publication Date

2019-11-01

DOI

10.1016/j.jnutbio.2019.108220

Peer reviewed

HHS Public Access

Author manuscript

J Nutr Biochem. Author manuscript; available in PMC 2020 November 01.

Published in final edited form as:

J Nutr Biochem. 2019 November ; 73: 108220. doi:10.1016/j.jnutbio.2019.108220.

Role of *microRNA-122* in Hepatic Lipid Metabolism of the Weanling Female Rat Offspring Exposed to Prenatal and Postnatal Caloric Restriction

Yun Dai, **Shubhamoy Ghosh**, **Bo-Chul Shin**, **Sherin U. Devaskar***

Department of Pediatrics and the Children's Discovery and Innovation Institute, David Geffen School of Medicine UCLA, Los Angeles, CA

Abstract

We examined the role of hepatocyte micro-RNA-122 and hypothalamic neuropeptides, in weanling (21d) female rats exposed to calorie restriction induced growth restriction either prenatally (IUGR), postnatally (PNGR) or both (IPGR) versus ad lib fed controls (CON). IUGR were hyperinsulinemic, hyperleptinemic and dyslipidemic with high circulating miR-122. In contrast, PNGR and IPGR displayed insufficient glucose, insulin and leptin amidst high ketones with a dichotomy in circulating miR-122 of PNGR<IPGR=CON. Examination of livers revealed a reduction in miR-122 expression in PNGR and IPGR reflecting the hepatic size. This reduction of hepatic miR-122 was associated with an increase in specific target transcripts (ALDO-A, BCKDK, PPAR-β) and those mediating fatty acid oxidation (PGC-1α, CPT-1α), with a concomitant suppression of fatty acid and cholesterol synthesizing transcripts (FAS, HMGCR). Functionally, these changes correlated with increased fatty acid oxidation and mitochondrial CPT1α enzyme activity ex-vivo. In-vitro physiologic (serum starvation) and genetic manipulation of miR-122 in H4IIE hepatoma cells revealed fidelity in regulating ALDO-A/BCKDK, but an infidelity in perturbing fatty acid/cholesterol synthesizing and oxidizing gene transcripts. Nevertheless, changes in endogenous miR-122 maintained singular directionality while altering FAS/HMGCR and CPT1α/PGC1α, almost reflecting each other, and thereby maintaining a balance in fatty acid/cholesterol supply necessary to meet the in-vitro demands of these rapidly proliferating transformed cells. Successive microarray based analysis, comparing IPGR to CON demonstrated differential expression of hypothalamic genes mediating cell proliferation and survival, appetite/energy balance, circadian rhythm and obesity/diabetes. We conclude that miR-122 regulates genes mediating fatty acid/cholesterol metabolism in postnatal female rats, fueling the energy demand.

*Address all correspondence to: 10833 Le Conte Avenue, MDCC-22-412, Los Angeles, CA 90095-1752, Phone No.: 310-825-5095, FAX No.: 310-206-4584, sdevaskar@mednet.ucla.edu.

The authors have no conflicts of interest.

Keywords

Intra-uterine growth restriction; microRNA-122; hepatic fatty acid synthesis; fatty acid oxidation; hypothalamic genes; energy balance; circadian rhythm

1. Introduction:

Unbalanced nutrition is a major cause for metabolic associated maladies. Occurrence of overweight among the children of developed countries and its association with type II diabetes mellitus and other metabolic syndromes implies a combination of factors, majority of which bear connections with nutritional intake during different phases of the life cycle [1]. The relevance of nutrition during pregnancy and early infancy in defining long-term effects on health and survival has been described earlier [2]. The Developmental Origins of Health and Disease (DoHaD) paradigm also provides a framework to assess the effect of early nutrition and growth on long-term health. This body of literature shows that early nutrition has significant consequences on later health and well-being [3–7].

Consistent with DoHAD, altered glucose and lipid metabolism with various metabolic maladies occur in animal models of prenatal caloric restriction. These dysregulations include fatty liver, increased hepatic cholesterol concentrations, upregulation of lipogenic genes [8] and downregulation of transcription factors like PPARα and PPARγ [9]. Increased lipogenesis may contribute to the increased adiposity in adult IUGR animal models, but also in children and human adults. In contrast, postnatal calorie and protein restriction or delayed “catch up growth” reversed development of obesity in IUGR animal models [10]. Reduction of fat mass and body weight was observed in maternal calorie restricted offspring exposed to postnatal calorie restriction in mice [11] and rats [12, 13]. Differential changes in glucose and fatty acid synthesizing regulatory genes such as hepatic fatty acid synthase (FAS), Sterol Regulatory Element Binding Protein 1c (SREBP-1c) and Phosphoenolpyruvate Carboxykinase (PEPCK) were noted at the adult stage [14]. However, the underlying mechanisms that alter transcription factors or genes that regulate triglycerides (TG), cholesterol and fatty acid homeostasis in the offspring, exposed to either prenatal or postnatal calorie restriction, have not been investigated at an early stage in life. Such changes if present early in life would provide credence to the concept of persistent changes in the adult offspring in response to early life events.

Lipid metabolism is closely controlled at the cellular level by classical transcriptional regulatory components of cholesterol metabolism, SREBP and Liver X Receptor (LXR) along with members of noncoding RNAs consisting of microRNAs (*miRNAs*) as one class of them [14, 15]. *miRNAs* are RNAs of 20–25 nucleotides size and are recognized as negative post-transcriptional regulators of genes. By binding to the complementary 3’-untranslated region (UTR) of messenger RNAs, microRNAs degrade target mRNAs or block translation. Several *miRNAs* are functionally involved in regulating the lipid metabolism, such as *miR-33, miR-122, miR-27a/b, miR-378, miR-34a* and *miR-21*. Of these *miRs*, *miR-122* is expressed with high prominence in developing and adult livers and has been reported to be a key regulator of hepatic fatty acid and cholesterol metabolism [15]. In

addition, *miR-122* has various other regulatory roles related to cellular senescence and stress response, circadian regulation of hepatic genes, iron metabolism, and propagation of specific hepatitis producing viruses. While *miR-122* promotes hepatic fatty acid synthesis in adult livers, in the IUGR offspring, when exposed to postnatal caloric restriction or of the female sex, there is a protection against developing adult onset obesity with the metabolic syndrome phenotype. Whether hepatic *miR-122* expression and its role in lipid biosynthesis are modified in response to IUGR with or without postnatal calorie restriction, or by the female sex, remains unexplored. Our previous investigations in the female IUGR offspring revealed perturbed milk and food intake patterns [16] suggestive of hypothalamic involvement [16]. Further, while we have previously observed that the metabolic phenotype of the male IUGR offspring with postnatal calorie restriction displays circadian dysregulation [17], the perturbed expression of hypothalamic genes including *miR-122* [18], associated with such hepatic dysregulation requires investigation. Therefore, in the present study, we hypothesized that hepatic fatty acid and cholesterol metabolism are adversely affected by reduced *miR-122* expression. This is in association with perturbed hypothalamic circadian genes and *miR-122*, responsive to postnatal calorie and thereby growth restriction (GR) by itself, or when superimposed on prenatal calorie restriction with IUGR, particularly in the female offspring at an early stage of development. In order to test this hypothesis, we separated the effects of prenatal (IUGR) versus postnatal (PNGR) and superimposed postnatal on prenatal calorie and thereby growth restriction (IPGR) in weanling female rats.

2. Material and methods

2.1. In vivo studies

2.1.1. Maternal Nutrition Restriction Model: Pregnant Sprague-Dawley rats received ~50% of their daily food intake beginning from gestation day 11 through day 21, causing caloric restriction during mid- to late pregnancy (~11g/day), compared to their control counterparts who received ad libitum rat chow (~22g/d) (Diet 7013 from Envigo, Madison, WI: Energy 3.1 kcal/kg, [calories from protein 23%, from fat 18%, and from carbohydrate 59%] crude protein 18%, fat [ether extract] 6.2%, carbohydrate 45%, crude fiber 4%, neutral detergent fiber 13.6% and ash 6.2%). Both groups accessed drinking water *ad libitum*. At birth, the litter size was culled to six. Four groups were created by cross-fostering with control mothers (~40g/d) rearing control pups (CON) or prenatally growth restricted pups (IUGR), and pre- and postnatal growth restricted mothers (~20g/d) rearing prenatally growth restricted pups (IPGR) or control pups (PNGR) (Figure 1). At day 21, the female pups were examined soon after weaning from the mother.

2.1.2. Body weight, organ weight and nose-tail length: Body weight, organ weight and nose-tail length were measured in 21d old animals from all four groups. The animals were first weighed and then deeply anesthetized by inhalation of isoflurane, nose-tail length was recorded and organs/tissues [brain, brown adipose tissue (BAT), pancreas, liver and skeletal muscle] were mechanically isolated and weighed individually.

2.1.3. Plasma Metabolites and Hormones/Growth factors: Plasma insulin and leptin were quantified by double antibody radioimmunoassays (Linco Research, St. Charles,

MO). In addition, serum triacylglycerol, cholesterol, high-density lipoprotein (HDL), unesterified cholesterol and free fatty acids were measured by colorimetric assays. Total plasma ketone bodies were measured with a commercial kit (Wako Diagnostics, Richmond, VA). Insulin-like growth factor 1 (IGF-1) measurement was conducted as previously described [19]. Briefly, serum samples were pre-extracted with acid/ethanol reagent (12.5% 2N HCl and 87.5% ethanol), neutralized with 1M Tris base and then diluted with assay buffer. In-house enzyme-linked immunoassays were used to measure rat IGF-1 concentrations. Ninety-six well microtiter plates were coated with capture antibody at pH 7.4, and incubated with serum samples at room temperature for 2 hours. The reaction was terminated by the addition of 50 μl of 2N H_2SO_4 and the absorbance was determined at 490 nm in an ELISA plate reader (Molecular Design, Sunnyvale, CA). The IGF-1 assay has a sensitivity of 0.1 ng/ml. The intra-assay and inter-assay coefficients of variation were <10% in the range from 1 to 10 ng/ml.

2.1.4. Hepatic Studies:

2.1.4.1. Western Blot Analysis: Western blot analysis was performed as previously described [16]. In brief, 50 μg of liver was homogenized in cell lysis buffer (Cell Signaling Technology, Danvers, MA), and was subsequently separated on SDS-PAGE, and electro-blotted onto nitrocellulose membranes. The membranes were incubated with Mouse fatty acid synthase (FAS) and acetyl CoA carboxylase (ACC) antibodies (BD transduction laboratories, San Jose, California) overnight at 4°C. Mouse anti-vinculin (Sigma, St. Louis, MO) was used as an internal loading control. The proteins were visualized in Typhoon 9410 Phosphorimager (GE Healthcare Biosciences, Piscataway, NJ) by blotting with enhanced chemiluminescence (ECL) Plus detection kit (GE Healthcare Biosciences) followed by quantification in Image Quant 5.2 software (GE Healthcare Biosciences) and normalized to vinculin.

2.1.4.2. Mitochondrial carnitine palmitoyl transferase 1α (CPT1α) Enzyme Activity: Fresh livers (450 mg) were isolated from CON, IUGR, IPGR and PNGR rats and placed in ice-cold mitochondria isolation buffer (300 mM sucrose, 1 mM EGTA, 5 mM HEPES, pH 7.4, 1 mg/ml BSA [20]. The livers were minced with scissors on ice and homogenized using four (up and down) strokes with a motor-driven pestle rotating at 550 rpm. The homogenates were centrifuged at 600 X g for 12 min. The pellets were then discarded and the supernatants collected and centrifuged at 6800 X g for 12 min. The supernatants were removed and the pellets re-suspended in mitochondria isolation buffer and centrifuged again at 12,000 X g for 12 min. The supernatants were discarded and the pellets re-suspended again in mitochondria isolation buffer. After centrifugation at 12,000 g for 12 min, the final pellets were re-suspended in a 1 ml mitochondria isolation buffer without EGTA. Palmitoyl-CoA was incubated with 100 μg of liver mitochondria enriched samples from four groups and 10 μl diluted L-[methyl-^{3}H] carnitine in assay buffer for 10 minutes, and 1-BuOH was used to extract the formed palmitoyl-carnitine.

2.1.4.3. Ex-vivo hepatic fatty acid oxidation: Fatty acid oxidation measurement was undertaken as described previously with some modifications [21]. Finely minced liver slices (~0.5 mm thick, ~150 mg) from freshly harvested livers of CON, IUGR, IPGR and PNGR

were placed in 25-ml glass vials fitted with center wells containing 2N NaOH and circular filter papers. Tissues were placed at the bottom of the vials in 2 ml of Krebs-Ringer buffer (pH 7.4) with 0.4% BSA and 1 μCi (57 mCi/mmol) of ^{14}C-palmitate (CFA-23; Amersham Biosciences). Vials were capped with a rubber septum, and contents of the vial were gassed with 100% O_2 for 10 minutes and incubated at 37°C for 2 hours on a rotatory shaker. Then, 2 ml of 6N HCl was injected to release $^{14}CO_2$. To ensure adequate transfer of $^{14}CO_2$ to the NaOH-soaked filter papers in the center wells, vials were left undisturbed overnight at room temperature. The filter papers were transferred into scintillation fluid and radioactivity assessed.

2.2. In vitro studies

2.2.1. Cell culture: The rat H4IIE (CRL-1548) hepatocyte cells (American Type Culture Collection; Manassas, VA, USA) were cultured in DMEM medium supplemented with 10% fetal bovine serum (FBS), 50 μg/ml streptomycin, 50 μg/ml penicillin G and 100 μg neomycin, and grown at 37°C with 5% CO_2.

2.2.2. Serum deprivation studies: H4IIE cells were cultured in serum-free DMEM for 24 h before they were collected for analysis.

2.2.3. Construction of 3′-UTR reporter plasmids: psiCHECK™−2 vector, a dual-luciferase plasmid harboring both the synthetic Firefly Luciferase (Fluc) gene (transfection control) and the synthetic Renilla Luciferase (hRluc) gene (reporter) was obtained from Promega (C8021, Madison, WI). A complementary target site for the *miR-122* seed sequence (*5′-CAAACACCATTGTCACACTCCA-3′*) was inserted between the XhoI–Not I restriction sites in the multiple cloning region of the 3'-UTR of the hRluc gene [22].

2.2.4. Luciferase reporter assay: H4IIE cells were seeded in 96-well plates containing antibiotic-free medium for 24h. On the day of transfection, cells were washed with PBS and switched to reduced serum medium (Invitrogen, Carlsbad, CA), and transfected with 100 ng/well of the engineered *miR122*-luciferase vector or empty plasmid using Lipofectamine 2000. Cells were grown at 37°C and harvested after transfection for luciferase and viability assays. Firefly and Renilla luciferase activities were measured using the Dual Luciferase Assay System (Cat.No. E1980, Promega, San Francisco, CA) [22]. Relative enzyme activity was expressed as a ratio of *Renilla*/Firefly luciferase.

2.2.5. Transfection of cells with *miR-122* Mimic, Inhibitor (Anti-*miR-122*), and respective negative control RNAs: H4IIE cells were transiently transfected with *miR-122* mimic (Dharmacon, Lafayette, CO) or *miR-122* inhibitor at two concentrations (40 nM or 60 nM, Dharmacon, Lafayette, CO) or their respective negative control RNAs, using Lipofectamine 2000 reagent (Invitrogen Life Sciences, Carlsbad, CA) following the manufacturer's protocol. After 24 or 48 h the cells were subjected to trypsin treatment and RNA was harvested for the subsequent Real time PCR assay.

2.2.6. Reverse Transcription and quantitative Real-Time Polymerase Chain Reaction quantification of *miR-122* from liver, H4IIE cells and plasma: Liver and

H4IIE cells: Small RNAs from liver or H4IIE cells were isolated with miRNeasy mini kit (Qiagen, Valencia, CA). Total RNA (10 ng) was reverse transcribed using the Taq-Man miRNA reverse-transcription kit and the TaqMan miRNA assay specific for *miR-122* according to the manufacturer's instructions (Applied Biosystems, Foster City, CA).

Plasma: Blood samples were collected in EDTA-containing tubes (BD vacutainer plus plastic, K_2EDTA) and plasma was isolated by centrifugation at 3000 g for 15 min at 4°C. Qiagen miRNeasy Mini kit (Cat #217184, Valencia, CA) was used to isolate total cell free RNA from plasma with modifications. Briefly, 1 ml of QIAzol lysis reagent was added to 200 μl of plasma followed by the same amount of chloroform, and phase separation was achieved by centrifugation at 12,000 *g* for 15 min at 4°C. Total RNA was isolated from the aqueous phase by submitting through RNeasy mini spin column. Total RNA (25 ng) was reverse transcribed using the Taq-Man miRNA reverse-transcription kit and the TaqMan miRNA assay specific for *miR-122* (Applied Biosystems, Foster, CA). Expression of mature *miR-122* was measured by the Taqman *microRNA* Assay (Applied Biosystems, Foster City, CA) specific for rno-*miR-122* (Applied Biosystem assay #4427975/002245) and *U6* snRNA (Applied Biosystem assay #4427975/001973) was used as an internal control. In addition, synthetic Ce-miR-39 (Applied Biosystem assay #4427975/000200) from *C. elegans* was used as a spike in control to normalize the relative concentration of plasma microRNA [23, 24].

2.2.7. Reverse Transcription and Quantitative Real-Time Polymerase Chain Reaction quantification of fatty acid metabolism gene transcripts and *miR-122* targeted *mRNAs*: Total RNA from liver or H4IIE cells was extracted by using an RNAeasy mini kit (Qiagen, Valencia, CA). First-strand cDNA was synthesized from 1 μg of DNase-treated total RNA using Superscript II reverse transcriptase (Invitrogen Life Technologies, Carlsbad, CA), as previously described [16]. Primers and Taqman probes for detection of metabolism and *miR-122* targeted genes are listed in Table 1A. Taqman probes were labeled with 5′-end fluorescent dye 6-carboxyfluorescein (FAM) and 3′-end fluorescent dye N,N,N′,N′-tetramethyl-6-carboxyrhodamine (TAMRA) (Applied Biosystems, Foster CA). Taqman PCR was carried out using an ABI prism 7700 sequence detector (Applied Biosystems, Foster, CA) and glyceraldehyde-3-phosphate dehydrogenase (GAPDH) (Applied Biosystems, Foster, CA) was used as the internal control. Relative quantification of PCR products was based on value differences between the target and GAPDH using the comparative Ct method, as previously described [16].

2.2.8. Hypothalamic studies: For these studies, only two experimental groups (CON and IPGR) were selected for analyses.

2.2.8.1. Microarray-based expression profiling of hypothalamus: Microarray Gene expression profiling was performed using the Affymetrix GeneChip Rat ToxFX1.0 Genome Arrays (Affymetrix, Santa Clara, CA). Total RNA was extracted from hypothalamus using the QIAGEN miRNeasy Mini kit (Qiagen, Hilden, Germany). The yield and RNA purity were determined spectrophotometrically (NanoDrop, Wilmington, DE) and by formaldehyde-agarose gel electrophoresis, as previously described [17]. Samples for array hybridization were prepared as described in the Affymetrix GeneChip® Expression

Technical Manual. Briefly, 1 μg of total RNA was used to synthesize double-stranded cDNAs with a GeneChip® Expression 30-Amplification Reagents One-Cycle cDNA Synthesis kit (Affymetrix, Santa Clara, CA). Biotin-labeled cRNAs were then synthesized from cDNAs using GeneChip® Expression 30-Amplification Reagents for *in-vitro* transcription (IVT) Labeling (Affymetrix, Santa Clara, CA). After fragmentation, the biotinylated cRNAs were hybridized to array in a GeneChip Hybridization Oven 645 at 45°C for 16h. The arrays were washed, stained, and scanned using Affymetrix Fluidics Station FS450 and GeneChip Scanner 3000 7G. Two independent replicated experiments were carried out for all treatments. The data was analyzed using the dCHIP software [25]. Pair-wise comparisons were made between CON and IPGR groups. Satisfactory image files were analyzed to generate probe intensity files.

2.2.8.2. Verification of microarray-based expression profiling by a quantitative RT-PCR: First strand cDNA was synthesized from 1 μg of DNase treated total RNA using Superscript II reverse transcriptase (Invitrogen Life Technologies, Carlsbad, CA) and quantitative real time PCR was performed as previously described [16, 26, 27]. Primers and Taqman probes for detection of specific genes in hypothalamus were designed using Primer Express Software (Applied Biosystems, Foster, CA) and are listed in Table 1B. These designed forward and reverse primers generated corresponding DNA fragments after amplification. Taqman probes were synthesized and labeled with fluorescent dye, 6-carboxyfluorescein (FAM) on the 5′-end and N,N,N′,N′-tetramethyl-6-carboxyrhodamine (TAMRA) on the 3′-end (Applied Biosystems, Foster CA). Taqman PCR was carried out using a StepOnePlus™ real-time PCR system (Applied Biosystems, Foster, CA). Real time PCR quantification was then performed using Taqman glyceraldehyde-3-phosphate dehydrogenase (GAPDH) or eukaryotic 18S rRNA (Applied Biosystems, Foster, CA) as internal controls. PCR amplifications were performed in triplicates. The amplification cycles consisted of 12 min at 95°C (hot start), followed by 40 cycles at 95°C for 30 sec (denaturation), <50°C for glial fibrillary acidic protein (GFAP); 55°C for Fujimycin or FK506 binding protein 5 (Fkbp5), zinc finger containing the BTB (br-c, ttk and bab) domain 16 (Zbtb16), insulin-like growth factor binding protein 3 (Igfbp3), hypocretin receptor 1 (Hcrtr1), hypocretin, Hcrt2, bone morphogenetic protein (Bmp4), Igfbp5 and Ceacam10; 58°C for neuropeptide Y (NPY); 60°C for RNA binding motif 3 (Rbm3), agouti-related peptide (AgRP), pro-opiomelanocortin (POMC), cryptochrome circadian regulator 2 (Cry2), period circadian regulator 2 (Per2), and circadian locomotor output cycles kaput (CLOCK) over 30 sec (annealing), and 72°C for 30 sec (extension), using reagents from Applied Biosystems (Foster, CA). Relative quantification of PCR products were based on value differences between the target and glyceraldehyde 3-phosphate dehydrogenase (GAPDH) or 18S ribosomal RNA (rRNA) control using the comparative C_T method, as previously described [16, 26, 27]. In addition, *miR-122* expression was also assessed employing the same reverse transcription and PCR conditions as described above for the liver.

2.3. Data Analysis:

Data are expressed as mean ± SEM. Inter-group differences were determined by the Fisher's paired least significant difference test when ANOVA revealed significance. When only two

groups were compared the Student's t-test was employed. Significance was achieved at P values ≤ 0.05.

3. Results:

3.1. Impact of early life caloric restriction on body weight, organ weight and lipid profile:

Although the birth weight of female IUGR pups was 88% of CON ($p<0.05$), total TG in IUGR was 1.2-fold higher compared to CON ($p<0.05$). However, no significant difference was observed in plasma cholesterol (both total and UC), HDL, free fatty acids (FFA) and glucose (Table 2A) concentrations. IUGR pups caught up, thus at 21d of age, body weight was similar to that of CON ($p>0.05$). In contrast to IUGR, the body weight of the other two groups remained low, i.e. IPGR was 27% and PNGR was 37% of CON ($p<0.05$ each). In addition IPGR was 26% and PNGR was 35% of IUGR body weight ($p<0.05$ each). No significant change was observed in nose-tail length and brain weight among the four groups of 21d old rats. Interestingly, IPGR and PNGR demonstrated significant decrease in BAT (20% and 23% of CON, 35% and 23% of IUGR, respectively, $p<0.05$ each) (Table 2B). A significant reduction in pancreatic weight was observed in IPGR and PNGR (both were 20% of CON and IUGR, respectively, $p<0.05$ each) (Table 2B). Similarly, liver weight of IPGR and PNGR were both 35% of CON and 37% of IUGR ($p<0.05$ each) (Table 2B). Substantial decrease was also observed in skeletal muscle weight of IPGR and PNGR groups (both 29% of CON and 25% of IUGR, $p<0.05$ each) (Table 2B). However, no significant differences in any organ weights were observed between CON and IUGR groups.

3.2. Influence of early life caloric restriction on plasma biomarkers:

Various plasma metabolites were measured in four 21d old experimental groups. Plasma glucose concentration was no different between CON and IUGR. In contrast, significant decrease was observed in IPGR and PNGR rats compared to CON ($p<0.05$ each). Plasma insulin observed in IPGR was 60% of CON ($p<0.05$) and 43% of IUGR ($p<0.05$). Similarly, plasma insulin in PNGR was 80% of CON ($p<0.05$) and 57% of IUGR ($p<0.05$). Plasma leptin concentration measured in IUGR was 1.8 fold higher compared to CON ($p<0.05$), while being undetectable in IPGR and PNGR (Table 2C). In addition, plasma IGF-1 concentrations were no different between IUGR and CON, but reduced in both the IPGR and PNGR groups versus both the IUGR and CON groups (Table 2C). Plasma total ketone bodies on the other hand were 2.9-fold higher in IUGR compared to CON ($p<0.05$), while IPGR and PNGR revealed 7.2 fold and 8.0 fold increase compared to CON ($p<0.05$ each) and 2.4 fold and 2.7 fold increase when compared to IUGR ($p<0.05$ each; Table 2C). Plasma TG in IUGR was similar to CON, in contrast, IPGR and PNGR revealed significantly reduced TG compared to CON ($p<0.05$ each) and IUGR ($p<0.05$ each). Plasma HDL demonstrated a similar pattern, with IPGR demonstrating 14% and 16% of CON ($p<0.05$) and IUGR ($p<0.05$), and PNGR being 16% and 15% of CON ($p<0.05$) and IUGR ($p<0.05$) respectively (Table 2C). While free fatty acids were increased by 45% in IUGR and IPGR, with a trend towards a reduction in PNGR versus CON, no significant inter-group changes were seen with total and UC Cholesterol concentrations (Table 2C).

3.3 Hepatic fatty acid metabolism during early life caloric restriction - IPGR and PNGR revealed increased fatty acid oxidation and decreased fatty acid synthesis:

In order to determine the energy utilization among caloric restricted groups we measured the expression of genes involved in lipid metabolism. Peroxisome proliferator activator receptor (PPAR)γ co-activator 1α (PGC-1α), the critical transcription factor of fatty acid oxidation in IPGR and PNGR was 3.5–3.6 fold higher than CON ($p<0.05$ each), and 2.6–2.7 fold higher in IPGR and PNGR than IUGR ($p<0.05$ each) (Figure 2A). Consistently, CPT-1α, the rate limiting enzyme of fatty acid oxidation, that transports FAs from cytosol to mitochondria, was 3.2 fold and 2.7 fold higher than CON ($p<0.05$ each) and IUGR ($p<0.05$ each) respectively (Figure 2B). CPT-1α enzyme activity using palmitoyl-CoA as the substrate was also enhanced in IPGR and PNGR compared to CON and IUGR (Figure 2C). Simultaneously, fatty acid oxidation rate in liver explants was significantly increased as well in IPGR and PNGR, as both of them were 1.5-fold higher than CON ($p<0.05$ each) and 2-fold higher than IUGR ($p<0.05$ each) (Figure 2D).

In contrast, FAS, one of the key enzymes that mediates fatty acid synthesis was significantly decreased in IPGR (7% of CON) and PNGR (7% of CON, $p<0.05$ each), (8% and 9% of IUGR respectively, $p<0.05$ each) (Figure 2E). The expression of FAS protein in IPGR and PNGR were also reduced significantly (11% and 13% of CON and IUGR, respectively, $p<0.05$ each) (Figure 2F). In contrast, ACC increased 2-fold in IUGR versus CON ($p<0.05$) with no differences seen in IPGR and PNGR when compared to CON (Figure 2G). Expression of 3-hydroxy-3-methyl-glutaryl-coenzyme A reductase (HMGCR), the rate limiting enzyme in cholesterol synthesis, was decreased in IPGR (13% of CON and IUGR, $p<0.05$ each) and PNGR (8% of CON and IUGR, $p<0.05$ each) (Figure 2H).

3.4. Hepatic *miR-122* expression altered in response to early life caloric restriction:

miR-122 has been shown to regulate fatty acid synthesis and fatty acid oxidation [14], thereby striking a balance in fatty acid metabolism by modifying genes such as FAS, CPT-1α and HMGCR. The expression of mature *miR-122* in IPGR was 20% of CON ($p<0.05$) and 17% of IUGR ($p<0.05$), similarly, PNGR was 44% of CON ($p<0.05$) and 38% of IUGR ($p<0.05$) (Figure 3A). The secreted *miR-122* concentrations in plasma were different from the corresponding liver *miR-122* expression, with IUGR displaying a trend towards a 1.6-fold increase and PNGR a 40% reduction ($p<0.05$), with no change observed in IPGR versus CON (Figure 3B). The decrease in hepatic *miR-122* expression in IPGR and PNGR was associated with a simultaneous increase in its reported target genes. Diacylglycerol O-acyltransferase 1 (DGAT1) was 3-fold more than in CON and 2-fold of that in IUGR (Figure 3C), aldolase A (ALDO-A) was ~1.5 fold more in IUGR, IPGR and PNGR than that of CON ($p<0.05$ each) (Figure 3D). Branched chain ketoacid dehydrogenase kinase (BCKDK) was ~1.4–1.7 fold greater in IUGR, IPGR and PNGR than in CON ($p<0.05$ each) (Figure 3E).

3.5. Endogenous *miR-122* reduces Renilla luciferase activity in rat H4IIE cells

We employed an experimental system of rat H4IIE hepatoma cells that previously demonstrated insulin sensitivity of the glucose and lipid metabolism [28]. Using these cells, we measured *miR-122*'s inhibitory activity on target mRNAs with the help of a dual

luciferase assay system. A complementary target site for *miR-122* seed sequence was sub-cloned at the 3'-end of the *hRluc* gene (Figure 4A). The theory being that any endogenous *miR-122* present will bind to its complementary target site of the seed sequence inserted in the 3'-UTR of the *hRluc* gene and post-transcriptionally decrease the luciferase enzyme activity. As such a huge reduction in luciferase activity upon transfection of the constructed *hRluc* gene in H4IIE cells was observed when compared with cells transfected with the empty vector (4% compared to Control; $p < 0.05$) (Figure 4B). Thus, we next examined the effects of serum starvation, *miR-122* overexpression and inhibition in these H4IIE cells.

3.6. Serum starvation in-vitro:

To mimic the *in-vivo* chronic caloric restriction in rats, *in-vitro* serum starvation over a shorter time-frame in H4IIE cells was undertaken. Consistent with our in-vivo results, *miR-122* expression in serum starved cells was 54% of CON ($p<0.05$) (Figure 5A). Simultaneously, ALDO-A, the reported target gene of *miR-122* in serum starved cells was 20% more than CON ($p<0.05$) (Figure 5B), PGC-1α was 3.8 fold higher in serum starved cells compared to CON ($p<0.05$) (Figure 5C). In addition, serum starvation increased CPT-1α expression by 20% compared to CON ($p<0.05$) (Figure 5D). PPAR-β, a potential target of *miR-122*, was also 20% higher in serum-starved cells versus CON cells (data not shown). Contrary to the in-vivo results, serum starvation in-vitro in H4IIE cells increased FAS mRNA by 50% (Figure 5E) and HMGCR mRNA by 20% compared to CON ($p<0.05$ each) (Figure 5F).

3.7. *miR-122* overexpression in-vitro using *miR-122* mimic:

Transfection efficiency of miRIDIAN *mimic* (Dharmacon) in H4IIE cells was evaluated using a transfection control construct containing the dye Dy-547 (Figure 6A). The transfection efficiency achieved was >90% (Figure 6B). Transient transfection of *miR-122* mimic at 15 nM, 25 nM and 40 nM doses over 24 hr resulted in a dose-dependent increase in *miR-122* expression. Based on these results, 40 nM was used as the final dose in subsequent experiments, where *miR-122* expression increased by 2.4 fold ($p<0.05$) compared to the transfection negative control (CON) (Figure 6B). Consistently, *miR-122* mimic decreased ALDO-A mRNA (80% of CON, $p<0.05$) (Figure 6C) and BCKDK mRNA (50% of CON, $p<0.05$) concentrations (Figure 6D). HMGCR and FAS expression increased in response to *miR-122* overexpression by 40% and 20% ($p<0.05$ each) respectively (Figure 6E,F), but PGC-1α and CPT-1α expression were also increased by 3.4-fold and 30% respectively, ($p<0.05$ each) (Figure 6G,H).

3.8. Inhibition of *miR-122* expression in-vitro using *miR-122* inhibitor:

Inhibition of *miR-122* by an inhibitor decreased endogenous *miR-122* expression to 47% of CON ($p<0.05$) (Figure 7A), which was associated with an increase in ALDO-A expression by 20% versus CON ($p<0.05$) (Figure 7B). Inhibition of *miR-122* expression also decreased HMGCR mRNA (82% of CON, $p<0.05$) (Figure 7C), and FAS mRNA (86% of CON) (Figure 7D). However in contrast to our *in-vivo* observations, reduced *miR-122* in-vitro was associated with decreased PGC-1α expression (74% of CON, $p<0.05$) (Figure 7E) with no change in CPT1α mRNA (90% of CON, $p>0.05$) (Figure 7F).

A summary of all the in-vivo and *in-vitro* experimental observations involving directional perturbations is provided in Table 3.

3.9. Identification of hypothalamic genes and their transcripts:

Microarray analysis of DNA reverse transcribed from extracted hypothalamic RNA obtained from two groups, namely the CON and IPGR revealed significant changes in various genes. An increase in the top 11 genes with a decrease in the bottom 12–26 genes in IPGR versus CON is seen (Figure 8A). Some of these changes were further validated by RT-PCR and a significant increase in Rbm3, AgRP, Fkbp5, Zbtb16, Npy, Igfbp3 and Hcrtr1 was observed in IPGR versus CON ($p<0.002$). In contrast, while no change was seen with Hcrt, Hcrt2 and Igfbp5, a reduction in Pomc, Bmp4 (trending down), GFAP and Ceacam 10 ($p<0.002$) was observed (Figure 8B). Next, we focused on circadian genes in particular, which revealed an increase in Cry1&2 and Per2&3 transcripts with the CLOCK transcript being equivocal in IPGR versus CON (Figure 8C). These observations were also validated by RT-PCR in the case of Cry2, Per2 and CLOCK transcripts ($p<0.006$) (Figure 8D). Further, similar to the liver, we observed a reduction in *miR-122* expression in the IPGR versus the CON group (Figure 8E), a gene that was undetectable by microarray analysis.

4. Discussion

We have for the first time, demonstrated changes in postnatal hepatic and plasma *miR-122* expression in the context of genes mediating fatty acid synthesis and oxidation, thereby regulating lipid metabolism. Our four experimental groups allowed distinction between IUGR exposed to adequate postnatal nutrition with catch-up growth from the poorly postnatal nourished PNGR and IPGR groups. The latter two groups demonstrated reduced body, liver, skeletal muscle, pancreas and brown adipose tissue weights at 21d of age. The IUGR group, at birth had high circulating triglyceride concentrations that remained so until 21d of age, along with elevated fatty acids (trend seen), insulin and leptin concentrations. These changes being consistent with the IUGR female being insulin and leptin resistant with dyslipidemia, all signs of early emergence of obesogenic tendencies and the metabolic syndrome. In contrast, the PNGR and IPGR groups displayed low body, liver, skeletal muscle, pancreas and brown adipose tissue weights with reduced plasma IGF-1, insulin, leptin, glucose, triglycerides and HDL cholesterol concentrations. These findings being consistent with early emergence of insulin and leptin sensitivity. Thus similar to the male counterpart [17], female IUGR offspring are prone for maladaptation when exposed to a normal postnatal diet following prenatal diet restriction, creating a mismatch in their nutritional environments. In contrast, a match of the intra-uterine and postnatal nutritional environments as encountered by the IPGR led to a lean and insulin/leptin sensitive phenotype, all emerging as early as in the weaning period of life.

In this phenotypic backdrop, exploration of hepatic *miR-122* expression revealed normalcy in the IUGR reflected so with a tendency towards elevation in plasma concentrations. Subsequently, a decrease of *miR-122* was seen in PNGR and IPGR livers reflected so in the plasma concentrations in the case of PNGR, while the IPGR plasma concentrations were no different from CON. Plasma *miR-122* has a translatable value to human infants with the

potential of serving as a biomarker for prenatal versus postnatal nutritional mismatch, where in the IUGR and PNGR groups that experience such a mismatch, the concentrations were perturbed. IUGR's elevation in plasma concentrations reflecting the catch-up growth experienced by the liver, while the reduction in PNGR reflecting the reduction in liver size (weight). In contrast, in CON and IPGR where a perinatal nutritional match exists, the plasma miR-122 concentrations appeared similar, despite a reduction in the IPGR's liver size. Interestingly, a positive correlation was previously observed between plasma FFA and *miR-122* concentrations [29]. Previously FFA have been observed to up-regulate the expression of hepatic *miR-122* in mouse or human hepatocellular carcinoma derived cell lines in a retinoic acid receptor-related orphan receptor-alpha (RORα) dependent manner [29], thereby enhancing the secretion of *miR-122* into the plasma. Plasma *miR-122* influences the lipid metabolism of peripheral non-hepatic tissues, thereby linking hepatic with peripheral tissue lipid metabolism. In our present study, the increased trend in plasma FFA concentrations observed in IUGR and IPGR groups may be commensurate with the increase in IUGR and IPGR plasma *miR-122* concentrations. The difference between IUGR and IPGR being the reliance of the former on an adequate supply of glucose, while the latter is dependent on ketones as a fuel supply. The PNGR group on the other hand unlike IPGR, revealed a lower trend in plasma FFA concentrations along with reduced plasma *miR-122* concentrations.

The reduction in hepatic *miR-122* concentrations in PNGR and IPGR was associated with an increase in transcripts of its previously determined key target genes, namely DGAT1, ALDO-A and BCKDK [29, 30]. This increase in target genes supports a functional relevance to the perturbed hepatic *miR-122* concentrations *in-vivo*. In addition, an association with reduced FAS and HMGCR expression in IPGR and PNGR supports a functional reduction in hepatic fatty acid and cholesterol synthesis in the presence of reduced hepatic *miR-122* expression. In contrast, an increase in hepatic CPT1α and PGC1α expression, both mediating different processes of fatty acid oxidation, along with enhanced mitochondrial CPT1α enzyme activity and fatty acid oxidation *ex-vivo*, further supports a biological relevance seen with long chain fatty acids serving as the primary fuel (due to a low glucose supply) in PNGR and IPGR more than in IUGR. The increase in plasma ketones in PNGR and IPGR > IUGR, further lends credence to lipid mobilization by the process of ketogenesis. Thus, our in-vivo/ex-vivo female early life rodent studies provide functional relevance to the observed perturbations in hepatic and plasma *miR-122* concentrations.

To further prove the mechanistic link between *miR-122* and fatty acid metabolizing genes, we resorted to *in-vitro* studies. To ensure adequate cellular transfection capabilities, we employed a rat hepatoma cell line, which is not completely reminiscent of a developing/ postnatal liver, having arisen from an adult rat, nevertheless regenerating with cell proliferation akin to the developing liver. With these caveats, we successfully achieved >90% transfection capability of exogenous reporter DNAs, and were able to manipulate endogenous *miR-122*, either increasing or reducing it by at least 50%. These changes demonstrated functional relevance, especially with opposing changes of the target complementary sequences as assessed by the reporter assay, and at least by 20% in previously established key endogenous target genes' expression [29, 30].

However, in contrast to our in-vivo/ex-vivo observations in early life weanling female livers, the rat hepatoma cells in-vitro for the most part revealed that perturbed *miR-122* was associated with changes in FAS/HMGCR and PGC1α/CPT1α expression that demonstrated the same directionality. Thus, elevated endogenous *miR-122* led to increased FAS/HMGCR and PGC1α/CPT1α expression, while a reduction of *miR-122* decreased these four genes' expression. This is despite having the appropriate opposing effect on target gene transcripts such as ALDO-A/BCKDK. Hepatoma cells being cancerous in nature require increased amount of fatty acids to meet the demand of rapid proliferation. Recent findings also suggested that cancer cells can utilize both lipogenic and lipolytic pathways to procure the necessary fatty acids required to fuel cellular metabolism [31, 32]. These changes in gene expression thus represent a modification necessary to survive under *in-vitro* conditions, where the culture media lacks fatty acids/ketones but rather contains high glucose concentrations (25 mM) capable of fueling intracellular lipid biogenesis and oxidation. This is unlike the *in-vivo* conditions encountered in PNGR and IPGR, where glucose availability is low while fatty acids/ketones availability remains adequate to high.

Regardless, serum starvation studies revealed a reduction in *miR-122* along with increased PGC1α/CPT1α similar to the *in-vivo* results, but unlike the *in-vivo* observations, increased rather than decreased FAS and HMGCR expression perhaps reflecting the excessive glucose availability in the media. This increase in FAS/HMGCR expression almost also keeping up with the increase in gene products mediating oxidation. However, when endogenous *miR-122* was genetically inhibited (rather than in response to serum starvation), ALDO-A increased as expected, and HMGCR and FAS expression was reduced as well. However, the reduction of FAS/HMGCR mRNAs was accompanied by an unexpected reduction in PGC1α/CPT1α expression. This change in PGC1α/CPT1α is unlike the PNGR/IPGR *in-vivo/ex-vivo* and the serum starvation *in-vitro* observations.

On the contrary, upon overexpressing miR-122 exogenously, while ALDO-A/BCKDK expression decreased as expected, FAS/HMGCR expression increased as well per expectations. However again conflicting with the change in FAS/HMGCR expression, an increase rather than a decrease in PGC1α/CPT1α mRNAs was observed. Thus, it is clear that the experimental paradigm worked well based on the expected changes in key target genes' expression (ALDO-A/BCKDK), employed as positive controls. In contrast, the changes in FAS/HMGCR versus PGC1α/CPT1α seem to reflect each other only *in-vitro* supporting a complex interactive network between *miR-122* and the direct and/or indirect regulatory effect upon transcripts that mediate the balance between fatty acid/cholesterol synthesis and fatty acid oxidation.

The other observation of a ~50% perturbed *miR-122* expression being associated with only a 20% change in target mRNAs signifies that other *miRs* may be involved as well in regulating the target mRNAs involved and/or *miR-122* is engaged in post-transcriptionally regulating a network of transcripts. Thus, future studies employing hepatic RNA-sequencing may uncover these networks of target genes and pathways involved. Our current studies have attempted to uncover the role of *miR-122* in the hepatic fatty acid/cholesterol metabolism during postnatal development. Our previous studies had revealed diurnal variations with perturbed hepatic circadian gene expression in male 21d old IPGR rats versus controls [17].

Subsequently, we undertook studies in the female 21d old IPGR rats and observed differences in hypothalamic genes, e.g. NPY, AgRP, POMC and CART engaged in appetite control [27]. Based on these prior studies, we next deemed it essential to undertake hypothalamic genome-wide studies of gene expression to determine the extent of changes that may be involved in regulating the hepatic lipid metabolism. While we validated our studies by RT-PCR, we were able to determine similar changes in NPY, AgRP and POMC as seen previously by us [16], serving as our experimental positive controls providing a double-check system, for our present studies. In addition, an increase in Rbm3 (anti-apoptosis and cell proliferation, proto-oncogene), FKbp5 (stress-related, cell proliferation/differentiation, related to type 2 diabetes and obesity), Zbtb16 (tumor suppressor) IgFbp3 (pre-diabetic, mediates cell proliferation/differentiation), Hcrtr1 (mediates hyperphagia), GFAP (hypothalamic glial activation stimulates NPY/AgRP inhibiting POMC) and Ceacam10 (mediates cell proliferation) was seen in IPGR. These changes support IPGR (PNGR superimposed on IUGR) displaying perturbed hypothalamic expression of appetite-controlling genes along with those that regulate cell proliferation/differentiation towards promoting cell survival necessary for this phenotype (PNGR-related), yet continuing to retain remnants of IUGR's propensity towards diabetes and/or obesity. Additional studies focused on circadian genes revealed an increase in specific transcripts in IPGR, namely Per2 and Cry2 with a tendency towards an increase in CLOCK expression. These findings in the hypothalamus are in keeping with prior studies demonstrating similar changes in the IPGR male livers [17], supporting a role for the hypothalamus in regulating the circadian clock relevant for hepatic metabolism. Disruption of the internal metabolic clock has a negative impact in predisposing towards metabolic disorganization subsequently [33]

Thus, the changes in the hypothalamus along with the changes in hepatic fat and cholesterol metabolic gene expression may set the stage for the adult phenotype. Along with various other regulatory mechanisms, post-transcriptional mechanisms involving various *miRs* play a key role in molding this phenotype. Previous in-vitro studies have shown that *miR-122* reduction employing antisense methodology is associated with an increase in pAMPK [18]. In the adult hypothalamus, a reciprocal relationship was observed between *miR-122* expression and pAMPK [18], which stimulates orexigenic peptides such as AgRP and NPY [34], both of which increased in the IPGR group of our present study. Although, we did not measure pAMPK in this study, a reduction in hypothalamic *miR-122* in the IPGR versus CON, is suggestive of increased pAMPK mediating the observed increase in AgRP and NPY. In addition, previous studies have demonstrated that IUGR reduces CPT1c in the hypothalamus, thereby reducing the central lipid sensing ability [35], perhaps explaining the noted dyslipidemia in the IUGR group in our present study.

The seeds of these phenotypes are sown prenatally, and are further modified by the postnatal nutritional environment. Thus, early determinants of aberrations in metabolic factors causing obesogenic tendencies are also evident in the female sex, having great repercussions on subsequent reproductive health with a potential effect on the next generation. In this paradigm, hepatic *miR-122* contributes towards the regulation of this ultimate phenotype of obesogenic tendencies observed in the female IUGR offspring, with partial amelioration in PNGR/IPGR.

Acknowledgments:

This work was supported by grants from the National Institutes of Health HD-41230 and HD-81206 (to SUD).

References:

[1]. Esposito K, Ciotola M, Maiorino MI, Giugliano D. Lifestyle approach for type 2 diabetes and metabolic syndrome. Curr Atheroscler Rep 2008;10:523–8. [PubMed: 18937901]

[2]. Tzanetakou IP, Mikhailidis DP, Perrea DN. Nutrition During Pregnancy and the Effect of Carbohydrates on the Offspring's Metabolic Profile: In Search of the "Perfect Maternal Diet". Open Cardiovasc Med J 2011;5:103–9. [PubMed: 21673843]

[3]. Wadhwa PD, Buss C, Entringer S, Swanson JM. Developmental Origins of Health and Disease: Brief History of the Approach and Current Focus on Epigenetic Mechanisms. Seminars in Reproductive Medicine 2009;27:358–68. [PubMed: 19711246]

[4]. Gruszfeld D, Socha P. Early nutrition and health: short- and long-term outcomes. World Rev Nutr Diet 2013;108:32–9. [PubMed: 24029784]

[5]. Larnkjaer A, Molgaard C, Michaelsen KF. Early nutrition impact on the insulin-like growth factor axis and later health consequences. Curr Opin Clin Nutr Metab Care 2012;15:285–92. [PubMed: 22466924]

[6]. Lucas A Programming by early nutrition: an experimental approach. J Nutr 1998;128:401S–6S. [PubMed: 9478036]

[7]. Robinson S, Fall C. Infant nutrition and later health: a review of current evidence. Nutrients 2012;4:859–74. [PubMed: 23016121]

[8]. Yamada M, Wolfe D, Han G, French SW, Ross MG, Desai M. Early onset of fatty liver in growth-restricted rat fetuses and newborns. Congenit Anom (Kyoto) 2011;51:167–73. [PubMed: 22103455]

[9]. Magee TR, Han G, Cherian B, Khorram O, Ross MG, Desai M. Down-regulation of transcription factor peroxisome proliferator-activated receptor in programmed hepatic lipid dysregulation and inflammation in intrauterine growth-restricted offspring. Am J Obstet Gynecol 2008;199:271 e1–5. [PubMed: 18667178]

[10]. Dai Y, Thamotharan S, Garg M, Shin BC, Devaskar SU. Superimposition of postnatal calorie restriction protects the aging male intrauterine growth-restricted offspring from metabolic maladaptations. Endocrinology 2012;153:4216–26. [PubMed: 22807491]

[11]. Hernandez-Valencia M, Patti ME. A thin phenotype is protective for impaired glucose tolerance and related to low birth weight in mice. Arch Med Res 2006;37:813–7. [PubMed: 16971218]

[12]. Choi GY, Tosh DN, Garg A, Mansano R, Ross MG, Desai M. Gender-specific programmed hepatic lipid dysregulation in intrauterine growth-restricted offspring. Am J Obstet Gynecol 2007;196:477 e1–7. [PubMed: 17466711]

[13]. Thompson NM, Norman AM, Donkin SS, Shankar RR, Vickers MH, Miles JL, et al. Prenatal and postnatal pathways to obesity: different underlying mechanisms, different metabolic outcomes. Endocrinology 2007;148:2345–54. [PubMed: 17272392]

[14]. Esau C, Davis S, Murray SF, Yu XX, Pandey SK, Pear M, et al. miR-122 regulation of lipid metabolism revealed by in vivo antisense targeting. Cell Metab 2006;3:87–98. [PubMed: 16459310]

[15]. Tsai WC, Hsu SD, Hsu CS, Lai TC, Chen SJ, Shen R, et al. MicroRNA-122 plays a critical role in liver homeostasis and hepatocarcinogenesis. J Clin Invest 2012;122:2884–97. [PubMed: 22820290]

[16]. Shin BC, Dai Y, Thamotharan M, Gibson LC, Devaskar SU. Pre- and postnatal calorie restriction perturbs early hypothalamic neuropeptide and energy balance. J Neurosci Res 2012;90:1169–82. [PubMed: 22388752]

[17]. Freije WA, Thamotharan S, Lee R, Shin BC, Devaskar SU. The hepatic transcriptome of young suckling and aging intrauterine growth restricted male rats. J Cell Biochem 2015;116:566–79. [PubMed: 25371150]

[18]. Kwon IG, Ha TK, Ryu SW, Ha E. Roux-en-Y gastric bypass stimulates hypothalamic miR-122 and inhibits cardiac and hepatic miR-122 expressions. J Surg Res 2015;199:371–7. [PubMed: 26130369]

[19]. Park JY, Cho MO, Leonard S, Calder B, Mian IS, Kim WH, et al. Homeostatic imbalance between apoptosis and cell renewal in the liver of premature aging Xpd mice. PLoS One 2008;3:e2346. [PubMed: 18545656]

[20]. McGarry JD, Mills SE, Long CS, Foster DW. Observations on the affinity for carnitine, and malonyl-CoA sensitivity, of carnitine palmitoyltransferase I in animal and human tissues. Demonstration of the presence of malonyl-CoA in non-hepatic tissues of the rat. Biochem J 1983;214:21–8. [PubMed: 6615466]

[21]. Cha SH, Hu Z, Chohnan S, Lane MD. Inhibition of hypothalamic fatty acid synthase triggers rapid activation of fatty acid oxidation in skeletal muscle. Proc Natl Acad Sci U S A 2005;102:14557–62. [PubMed: 16203972]

[22]. Vermeulen A, Robertson B, Dalby AB, Marshall WS, Karpilow J, Leake D, et al. Double-stranded regions are essential design components of potent inhibitors of RISC function. RNA 2007;13:723–30. [PubMed: 17400817]

[23]. Fichtlscherer S, De Rosa S, Fox H, Schwietz T, Fischer A, Liebetrau C, et al. Circulating microRNAs in patients with coronary artery disease. Circ Res 2010;107:677–84. [PubMed: 20595655]

[24]. Kroh EM, Parkin RK, Mitchell PS, Tewari M. Analysis of circulating microRNA biomarkers in plasma and serum using quantitative reverse transcription-PCR (qRT-PCR). Methods 2010;50:298–301. [PubMed: 20146939]

[25]. Li C, Wong WH. Model-based analysis of oligonucleotide arrays: expression index computation and outlier detection. Proc Natl Acad Sci U S A 2001;98:31–6. [PubMed: 11134512]

[26]. Thamotharan M, Shin BC, Suddirikku DT, Thamotharan S, Garg M, Devaskar SU. GLUT4 expression and subcellular localization in the intrauterine growth-restricted adult rat female offspring. Am J Physiol Endocrinol Metab 2005;288:E935–47. [PubMed: 15625086]

[27]. Gibson LC, Shin BC, Dai Y, Freije W, Kositamongkol S, Cho J, et al. Early leptin intervention reverses perturbed energy balance regulating hypothalamic neuropeptides in the pre- and postnatal calorie-restricted female rat offspring. J Neurosci Res 2015;93:902–12. [PubMed: 25639584]

[28]. Hectors TL, Vanparys C, Pereira-Fernandes A, Knapen D, Blust R. Mechanistic evaluation of the insulin response in H4IIE hepatoma cells: new endpoints for toxicity testing? Toxicol Lett 2012;212:180–9. [PubMed: 22652326]

[29]. Chai C, Rivkin M, Berkovits L, Simerzin A, Zorde-Khvalevsky E, Rosenberg N, et al. Metabolic Circuit Involving Free Fatty Acids, microRNA 122, and Triglyceride Synthesis in Liver and Muscle Tissues. Gastroenterology 2017;153:1404–15. [PubMed: 28802563]

[30]. Elmen J, Lindow M, Silahtaroglu A, Bak M, Christensen M, Lind-Thomsen A, et al. Antagonism of microRNA-122 in mice by systemically administered LNA-antimiR leads to up-regulation of a large set of predicted target mRNAs in the liver. Nucleic Acids Res 2008;36:1153–62. [PubMed: 18158304]

[31]. Nomura DK, Long JZ, Niessen S, Hoover HS, Ng SW, Cravatt BF. Monoacylglycerol lipase regulates a fatty acid network that promotes cancer pathogenesis. Cell 2010;140:49–61. [PubMed: 20079333]

[32]. Zaidi N, Lupien L, Kuemmerle NB, Kinlaw WB, Swinnen JV, Smans K. Lipogenesis and lipolysis: the pathways exploited by the cancer cells to acquire fatty acids. Prog Lipid Res 2013;52:585–9. [PubMed: 24001676]

[33]. Potter GD, Skene DJ, Arendt J, Cade JE, Grant PJ, Hardie LJ. Circadian Rhythm and Sleep Disruption: Causes, Metabolic Consequences, and Countermeasures. Endocr Rev 2016;37:584–608. [PubMed: 27763782]

[34]. Fukami T, Sun X, Li T, Desai M, Ross MG. Mechanism of programmed obesity in intrauterine fetal growth restricted offspring: paradoxically enhanced appetite stimulation in fed and fasting states. Reprod Sci 2012;19:423–30. [PubMed: 22344733]

[35]. Puglianiello A, Germani D, Antignani S, Tomba GS, Cianfarani S. Changes in the expression of hypothalamic lipid sensing genes in rat model of intrauterine growth retardation (IUGR). Pediatr Res 2007;61:433–7. [PubMed: 17515867]

Highlights:

- IUGR female weanling rats are hyperinsulinemic, hyperleptinemic and dyslipidemic setting them up for subsequent obesity/diabetes
- miR-122 regulates fatty acid and cholesterol synthesis along with fatty acid oxidation in weanling rat livers towards meeting the energy demands
- Perturbed plasma miR-122 may serve as an indicator of mismatched prenatal versus postnatal nutritional status during early development
- Hypothalamic miR-122 expression is downregulated in postnatal calorie restriction superimposed on intra-uterine calorie restricted weanling rats, with a reciprocal increase in orexigenic AgRP and NPY neuropeptides, thereby mediating the subsequent development of hyperphagia.
- Hypothalamic neuropeptides in postnatal calorie restriction superimposed on intra-uterine calorie restricted weanling rats reflect changing cell proliferation and survival, appetite/energy balance, circadian rhythm with a tendency of developing obesity/diabetes.

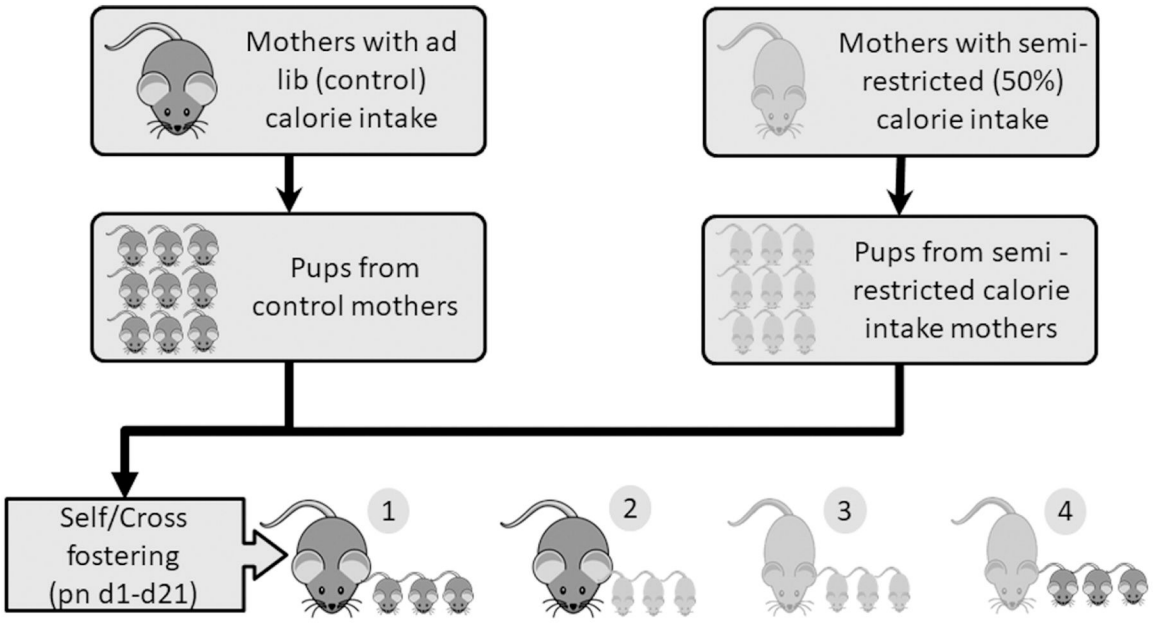

	CON	IUGR	IPGR	PNGR
Prenatal caloric restriction	-	+	+	-
Postnatal caloric restriction	-	-	+	+

Fig 1.

Study design.

Cartoon depicting the four experimental groups obtained by cross-fostering postnatal rat pups. 1) Control rats (CON), i.e. control mothers rearing control pups, 2) Intrauterine calorie restricted pups (IUGR), i.e. CON mothers rearing prenatal calorie restricted pups, 3) intrauterine and postnatal calorie restricted rats (IPGR), *i.e.* prenatal and postnatal calorie restricted mothers rearing prenatal calorie restricted pups, 4) postnatal calorie restricted rats (PNGR), *i.e.* control mothers exposed to postnatal calorie restriction rearing control pups.

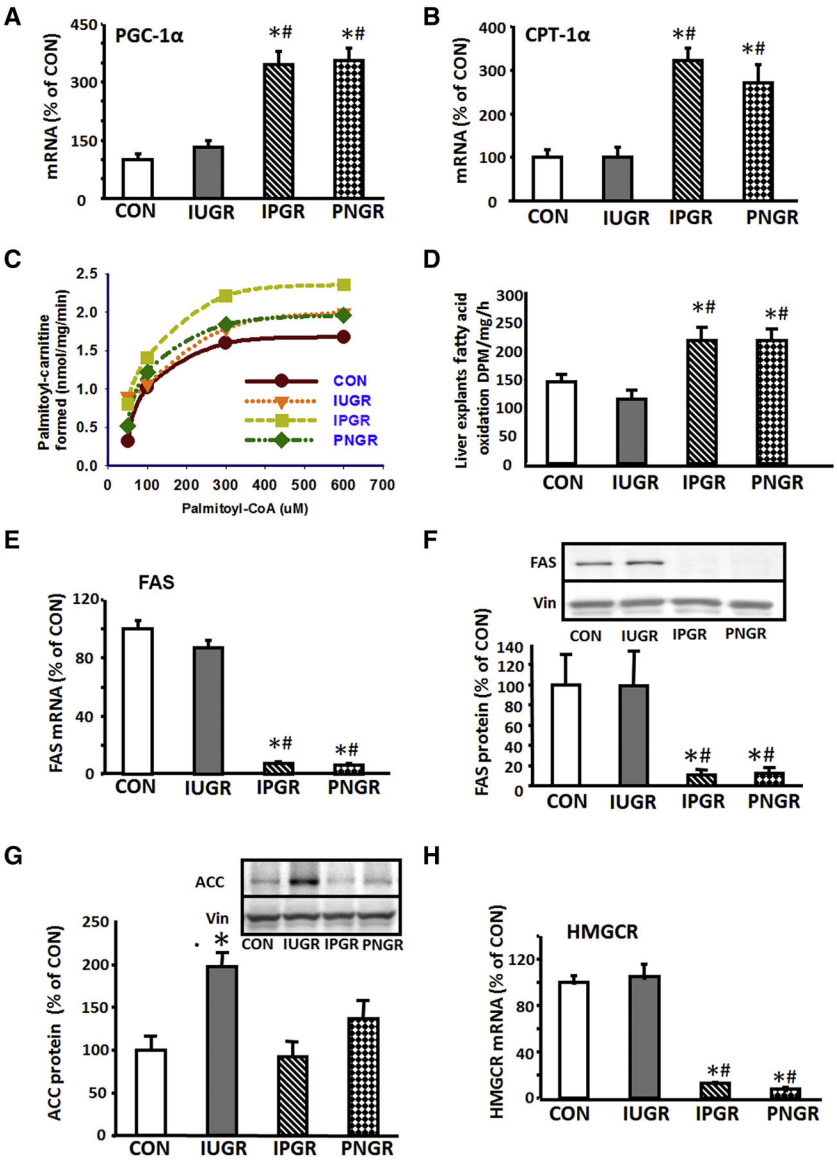

Fig 2.

In-vivo hepatic lipid metabolizing gene expression and function in experimental groups. **A**. PGC-1α mRNA concentration was significantly increased in both IPGR and PNGR groups compared to CON and IUGR, *#p<0.05 versus CON and IUGR in both groups, IUGR exhibited a similar PGC-1α concentration to that of CON (p>0.05). **B.** CPT-1α mRNA concentration was significantly increased in IPGR and PNGR groups compared to CON and IUGR. *#p<0.05 versus CON and IUGR in both groups, IUGR exhibited a similar CPT-1α concentration compared to CON (p>0.05). **C.** Mitochondrial CPT1α enzyme activity is depicted in a time-dependent manner. IUGR and PNGR demonstrated higher activity when compared to CON, with IPGR exhibiting the highest activity overall. **D.** Fatty acid oxidation in IPGR and PNGR were significantly increased compared to CON and IUGR, *#p<0.05 versus CON and IUGR in both groups. **E-F.** FAS mRNA concentration (**E**) and FAS protein (inset shows representative Western blots with vinculin as the internal

control) (**F**) were both significantly decreased in IPGR and PNGR groups pared to CON and IUGR, *#p<0.05 versus CON and IUGR for mRNA and protein in both groups, IUGR exhibited a similar FAS mRNA (**E**) and protein (**F**) concentration compared to CON (p>0.05). n=6 in each group for all measurements. **G.** Acetyl CoA carboxylase protein was increased in IUGR versus CON (*p<0.05; inset demonstrates representative Western blots with vinculin as the internal control). **H.** HMGCR mRNA concentration was significantly decreased in IPGR and PNGR groups compared to CON and IUGR, *#p<0.05 versus CON and IUGR in both groups, IUGR exhibited a similar HMGCR concentration compared to CON (p>0.05).

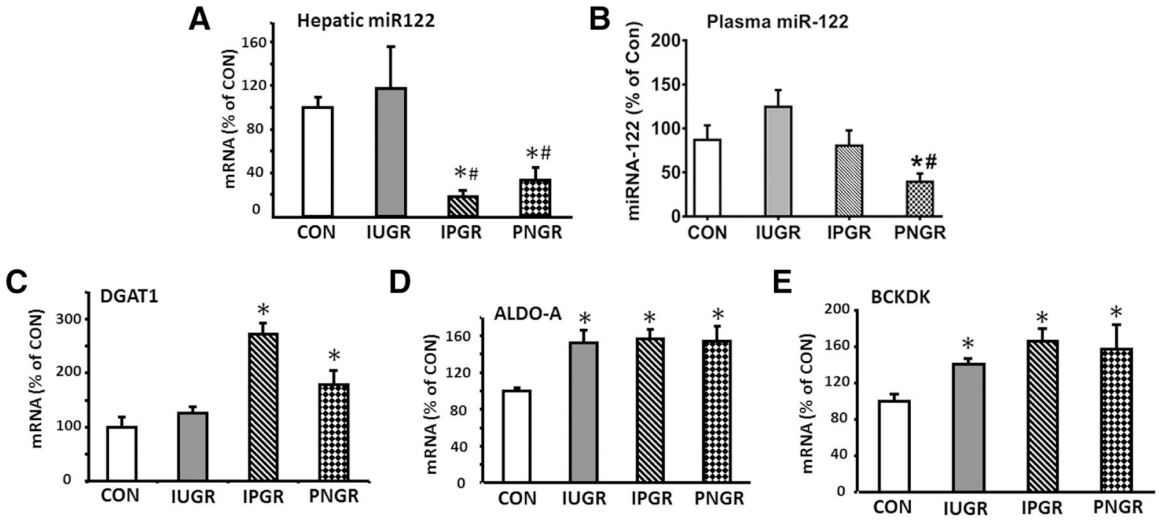

Fig 3:

Hepatic and Plasma miR-122 mRNA and its hepatic target gene expression.

A. Hepatic miR-122 mRNA was significantly decreased in IPGR and PNGR compared to CON and IUGR,*#$p<0.05$ versus CON and IUGR in both groups, miR-122 mRNA in IUGR was similar to CON ($p>0.05$). **B.** Plasma miR-122 mRNA was no different (to elevated) in IUGR and reduced in PNGR compared to CON and IPGR, *$p< 0.05$ versus CON and IPGR, $^{\#}p<0.05$ versus IUGR, with n=6 in each group. **C-E.** IPGR and PNGR revealed increased mRNA of miR-122 target genes DGAT1 (**C**), ALDO-A (**D**) and BCKDK (**E**) compared to CON (*$p<0.05$ each), while IUGR demonstrated a similar expression of DGAT1 (**C**) compared to CON (*$p>0.05$), but increased ALDO-A (**D**) and BCKDK (**E**) mRNAs compared to CON (*$p<0.05$ each)

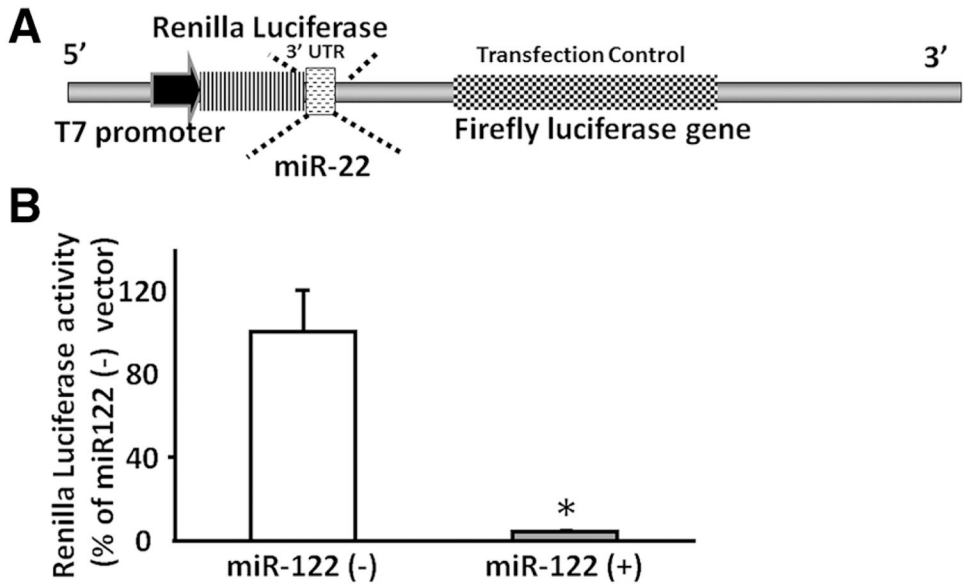

Fig 4.

In-vitro study of miR-122 functional activity. **A.** Structure of the engineered miR-122 3′UTR reporter plasmids: psiCHECK™-2 vector is a dual-luciferase plasmid containing both the synthetic Firefly Luciferase (Fluc) gene and the synthetic Renilla Luciferase (hRluc) gene. The complementary target sequences of miR-122 seed sequence (*5′CAAACACCATTGTCACACTCCA3′*) were inserted between the XhoI–NotI restriction sites in the multiple cloning region of the 3′ UTR of the hRluc gene. Functional activity of endogenous miR-122 is reflected as the luciferase activity emanating from the reporter hRluc gene (reporter) with Fluc acting as the transfection control.

B. The endogenous miR-122 in H4IIE cells annealing with its complementary seed sequences inserted in the 3′ UTR of the hRluc gene significantly decreased Renilla Luciferase activity, (*$p<0.05$ versus miR-122 (−) vector), n=6 in each group.

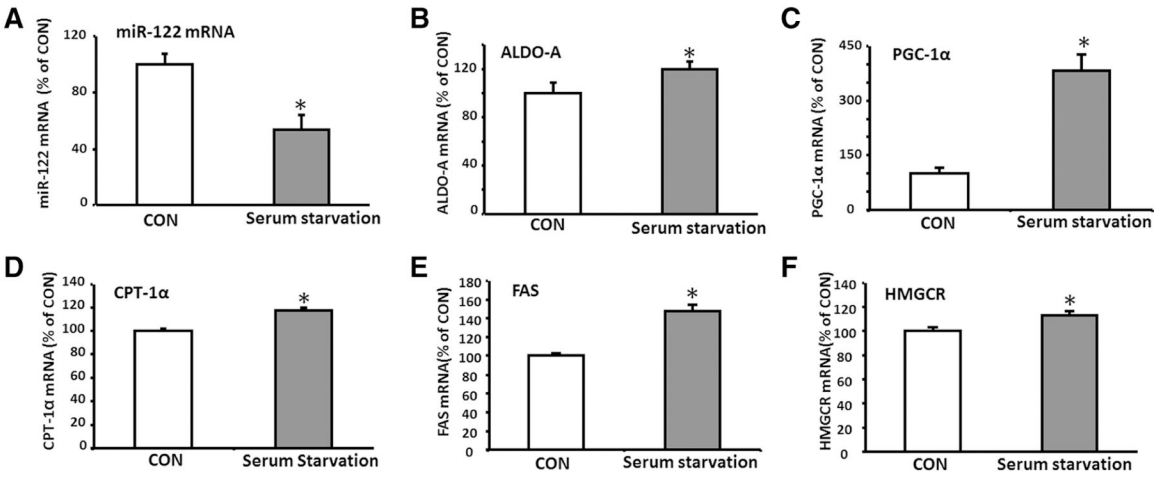

Fig 5:

In-vitro serum starvation of H4IIE cells.

Serum starvation of H4IIE cells for 24 hr decreased miR-122 mRNA (**A**) and increased miR-122 target gene ALDO-A expression (**B**), fatty acid oxidation mediators PGC-1α mRNA (**C**) and CPT-1α (**D**) expression, and lipid synthesizing FAS (**E**) and HMGCR expression (**F**) compared to CON cells maintained in serum (*p<0.05 versus CON). N=6 in each group and for each measurement.

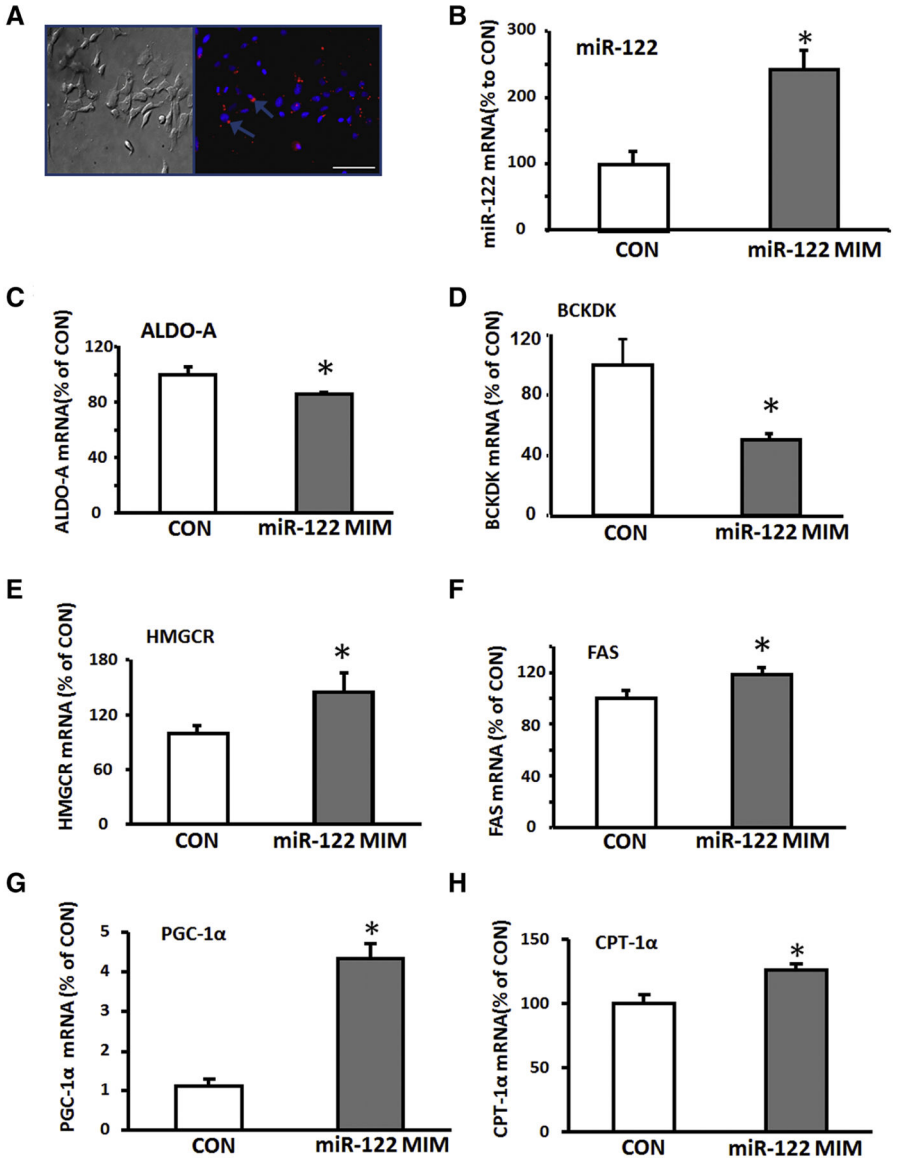

Fig 6.

In-vitro over-expression of miR-122 in H4IIE cells.

Normarski imaged photomicrograph of H4IIE cells employed for transfection of miR-122 related sequences (**A**, left panel). Representative photomicrograph shows transfection efficiency of miRIDIAN mimic (Dharmacon) using its transfection control plasmid containing dye Dy-547 (seen as red staining in **A**, right panel). Transfection of miR-122 mimic at 40 nM versus scrambled sequences (CON) increased miR-122 mRNA expression, *p<0.05 versus CON (**B**), and consequently decreased target genes ALDO-A (**C**) and BCKDK (**D**) gene expression (*p<0.05 versus CON), while increasing HMGCR (**E**), FAS (**F**) and PGC-1α (**G**) and CPT-1α (**H**) mRNAs (*p<0.05 versus CON). N=6 for each group and for each measurement.

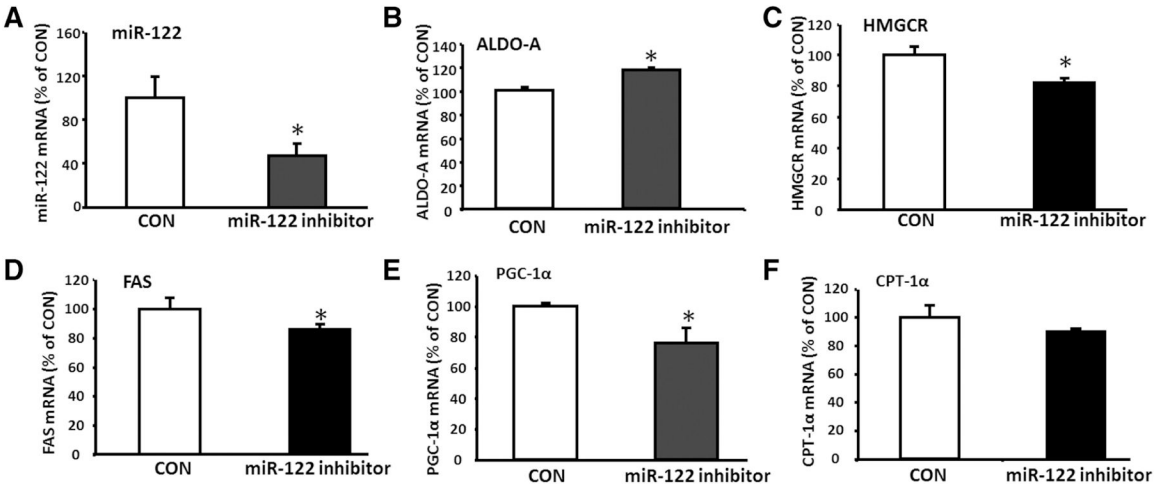

Fig 7.

In-vitro inhibition of miR-122 in H4IIE cells Transient transfection of miR-122 stem loop inhibitor versus empty vector (CON) decreased endogenous miR-122 mRNA (**)***p<0.05 versus CON, (**A**) and simultaneously increased miR-122 target gene ALDO-A mRNA (**B**), *p<0.05 versus CON. Specific inhibition of miR-122 decreased HMGCR (**C**), FAS (**D**) and PGC-1α (**E**) mRNAs, *p<0.05 versus CON for each of them, while not affecting CPT-1α mRNA (**F**, p>0.05). N=6 for each group and each measurement.

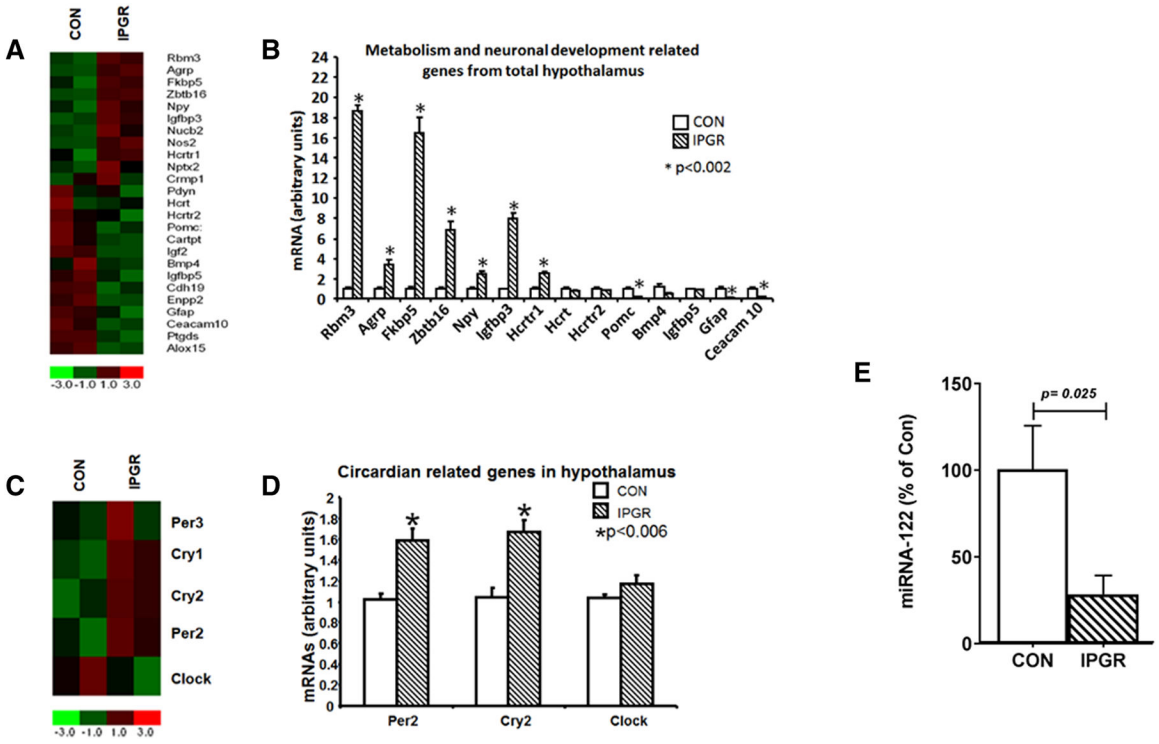

Fig 8.

Hypothalamic genes: Expression profiles of 21d CON and IPGR females. Heatmap showing the transcriptional profile of differentially expressed genes. The color code at the bottom displays fold change of gene expression (**A**). RT-PCR validation of expression of hypothalamic genes' expression related to metabolism in CON and IPGR female rats. Increased expression of Rbm3, Agrp, Fkbp5, Zbtb16, Npy, Igbp3 and Hcrtr1gene expression was observed in IPGR compared to CON, while expression of Pomc, Gfap and Ceacam 10 genes was decreased (**B**). Heatmap showing differentially expressed hypothalamic circadian rhythm associated genes in 21d CON and IPGR females (**C**). RT-PCR validation of hypothalamic genes' expression associated with circadian rhythm. The expression of Per2 and Cry2 genes was increased in IPGR compared to CON. *p<0.05 versus CON (**D**). RT-PCR quantification of hypothalamic *miR-122* expression demonstrates a decrease in IPGR compared to CON. *p=0.025 versus CON (**E**). n=6 in each group for each measurement.

Table 1A:

Primers and probes of miR-122 target genes and other genes influenced by miR-122 expression.

	Primer	Probe
ALDO A NM012495	F ATGGCAACCGTCACAGCACTTCG	CGAACAGTGCCCCCTGCCGT
	R GACAGGAAAGTGACCCCA	
BCKDK NM019244	F GCTGCCCGTTTCCCCT	CATTCCTATGCCGCTGGACTATATCCTGC
	R GGCGTTCTTGAGCAGCTCAG	
DGAT1 NM053437	F CTTTCTTCCTACCGGGATGTCA	TCTGTGGTGCCGCCAGCGAA
	R CAGACACAGCTTTGGCCTTG	
CPT1a NM031559	F CACTGGCCGAATGTCAAGC	ACGAAGAACATTGTGAGCGGCGTCC
	R CCCAGAGCCCTGTACCAAAG	
PGC-1α NM031347	F GCGCCAGCCAACACTCA	CTACAATGAATGCAGCGGTCTTAGCACTCA
	R TGGGTGTGGTTTGCATGGT	
HMGCR NM013134	F ATCAGCTGTACCATGCCGTCT	ATCGGAACCGTGGGTGGTGGG
	R AGGCTTGCTGAGGTAGAAGGTTG	
FAS NM017332	F ACGGCATTACTCGGTCCCTGTGT	TTCCGCCAGAGCCCTTTGTTAATTGGC
	R GTGTCCCATGTTGGATTTGGT	

F = forward, R = reverse.

Table 1B:

List of primers and probes of hypothalamic genes targeting qPCR analysis.

Target Gene	Primer	Probe
Rbm3 (NM053696)	F 5'TTTGGCTTCATCACCTTCAC 3'	5'AGCATGCCTCCGATGCCATG 3'
	R 5'CATCCAGGGACTCTCCATTC 3'	
AgRP (AF206017)	F 5'GCAGAGGTGCTAGATCCAC AGAA 3'	5' CGAGTCTCGTTCTCCGCGTCG 3'
	R 5'AGGACTCGTGCAGCCTTAC AC 3'	
Fkbp5 (NM001012 174)	F 5'GAATCCTGGGAGATGGACA C 3'	5' TGACAATGGCAGCCTGCTCCA 3'
	R 5' CCTCCCTTGAAGTACACCGT 3'	
Zbtb16 (NM001013 181)	F 5' AGTGTAATGGCTGTGGCAAG 3'	5' CAAGCACCAGCTGGAGACGCA 3'
	R 5' CTCACCTGTGTGAACCCTGT 3'	
NPY (M20373)	F 5' AATCTCATCACCAGACAGAG ATATGG 3'	5' AAGAGATCCAGCCCTGAGACACTG ATTTCA3'
	R 5' CATTTTCTGTGCTTTCTCTCA TTAAGA 3'	
Igfbp3 (NM012588)	F 5' TTCCATCCACTCCATTCAAA 3'	5' TGGCTGTCCCTAGCCTGGCC 3'
	R 5' GGCAGGGACCATATTCTGTC3 '	
Hcrtr1 (NM013064)	F 5' ACAACTTCCTCAGTGGCAAA 3'	5' CTGCTGCCTGCCTGGTCTGG 3'
	R 5' GACTTGTGTCTGGCAGAGGA 3'	
Hypocretin (NM013179)	F 5' ATACCATCTCTCCGGATTGC 3'	5' TCCCTGAGCTCCAGACACCATGA
	R 5' GCCCAGGGAACCTTTGTAG 3'	

Target Gene	Primer	Probe
Hcrtr2 (NM013074)	F 5' CTCTGGTGCAGACAGATTCC 3'	5' AAATGGAAGCAGCCGCAGCC 3'
	R 5' TTTATCTCAGCAGCGACAGC 3'	
POMC (AH002232)	F 5' ATAGACGTGTGGAGCTGGTGC 3'	5' CAGCCAGTGCCAGGACCTCACCAC 3'
	R 5' GCAAGCCAGCAGGTTGCT 3'	
Bmp4 (NM012827)	F 5' CCGGATTACATGAGGGATCT 3'	5' CCTGAGCGTCCTGCCAGCAG 3'
	R 5' CCAGATGTTCTTCGTGATGG 3'	
Igfbp5 (NM012817)	F 5' CAAGAGAAAGCAGTGCAAGC 3'	5' CCGCAAACGTGGCATCTGCT 3'
	R 5' GGCAGCTTCATCCCAxsTACTT 3'	
Gfap (NM017009)	F 5' TTTCTCCAACCTCCAGATCC 3'	5' CCGCATCTCCACCGTCTTTACCA 3'
	R 5' CTCCTTAATGACCTCGCCAT 3'	
Ceacam10 (NM173339)	F 5' CTACTGCTCACAGCCTCACTTT 3'	5' TGGAGCCCTCTCACCACTGCC 3'
	R 5'CACAGCGTCTACGGTGACTT 3'	
Cry2 (NM133405)	F 5' GGTCCGGGTATTTGATGAGT 3'	5' AGCCACATCCAGCTGCCTGC 3'
	R 5' GCAGTGGAAGAACTGTTGGA 3'	
Per2 (NM031678)	F 5' TCGACGTAACAGGGTGTGTT 3'	5' CCCAGGGAAGGACTGTCTTCCTCA 3'
	R 5' TCCTCTTTGGCTTCTGAGGT 3'	
Clock (NM021856)	F 5' AGGCATGTCACAGTTTCAGC3'	5' CATGCGTGTCCGCTGCTCTAGC3'
	R 5' CTTCTTGCTGCCGATGAATA3'	

F = forward, R = reverse.

Table 2A:

Body weights and plasma metabolites at day 2 in Control and IUGR female pups.

	Birth weight (g)	TG (mg/dl)	Cholesterol (mg/dl)	HDL (mg/dl)	UC (mg/dl)	FFA (mg/dl)	Glucose (mg/dl)
CON	7.4 ± 0.1	40.1± 1.6	70.8 ± 1.4	9.7 ± 1.9	22 ± 1.5	10.2 ± 0.5	74.8 ± 2.5
IUGR	6.5 ± 0.1	49.8 ± 2.6 *	75.8 ± 2.9	8. 7 ± 1.6	26 ± 2.4	11.3 ± 0.6	73.3 ± 1.9

N=6 in each group, ND= not detectable

* $p<0.05$ versus CON.

Table 2B:

Body and Organ weights and nose-tail Length of 21d females from all four groups.

	CON (6)	IUGR (6)	IPGR (6)	PNGR (6)
Body Weight (g)	55.2 ± 0.9	57.2 ± 0.8	14.8 ± 0.4 *#	20.2 ± 0.3 *#
N-T Length (cm)	18.5 ± 0.2	18.8 ± 0.2	15.2 ± 0.2	14.8 ± 0.3
Brain (g)	1.4 ± 0.01	1.3 ± 0.02	1.2 ± 0.01	1.2 ± 0.01
BAT (g)	0.3 ± 0.01	0.2 ± 0.02	0.06 ± 0.00 *#	0.07 ± 0.01 *#
Pancreas (g)	0.2 ± 0.02	0.2 ± 0.02	0.04 ± 0.00 *#	0.04 ± 0.00 *#
Liver (g)	2.0 ± 0.1	1.9 ± 0.1	0.7 ± 0.02 *#	0.7 ± 0.02 *#
Skeletal muscle (g)	0.7 ± 0.03	0.8 ± 0.1	0.2 ± 0.02 *#	0.2 ± 0.02 *#

N=6 in each group

*p<0.05 versus CON

#p<0.05 versus IUGR.

Table 2C:

Plasma metabolite and hormone/growth factor concentrations in 21d females of four experimental groups.

	CON	IUGR	IPGR	PNGR
IGF-1 (ng/ml)	318 ± 39.3	352 ± 29.3	27.2 ± 2.7 *#	32.2 ± 5.4 *#
Insulin (ng/ml)	0.5 ± 0.04	0.7 ± 0.07 *	0.3 ± 0.01 *#	0.4 ± 0.02 #
Leptin (ng/ml)	5.3 ± 0.3	9.6 ± 1.2 *	ND	ND
Glucose (mg/dl)	153.3 ± 8.7	137.3 ± 21.0	89.2 ± 7.8 *	101.5 ± 4.4
TG (mg/dl)	38.0 ± 2.7	43.5 ± 5.0 *	12.7 ± 1.9 *#	11.3 ± 1.3 *#
HDL (mg/dl)	42.2 ± 3.4	36.8 ± 13.7	5.7 ± 0.3 *	5.5 ± 0.3 *
FFA (mg/dl)	6 ± 0.4	8.5 ± 2.7	8.7 ± 1.0	3.5 ± 0.3
Cholesterol (mg/dl)	122.2 ± 5.6	125 ± 20.0	121.3 ± 28.7	181.3 ± 13.2
UC (mg/dl)	40.5 ± 1.7	41.8 ± 5.9	45.2 ± 9.4	62.75 ± 4.4
Ketone bodies (plasma) (μmol/L)	163.1 ± 28.0	480.4 ± 26.7 *	1171.6 ± 77.7 *#	1303.8 ± 135.6 *#

N=6 in each group

* $p<0.05$ versus CON

# $p<0.05$ versus IUGR.

Table 3:

Summary of *in vivo* results obtained in 21d females and *in vitro* results in H4IIE cells, respectively, showing the directionality of expression change in miR-122, ALDO-A, Fatty acid synthesis and Fatty acid oxidation enzymes in-vivo in PNGR/IPGR groups compared to CON, and in-vitro during serum starvation, miR-122 inhibition or overexpression versus their respective experimental controls.

	miR-122	**ALDO-A**	**Fatty acid synthesis**		**Fatty acid oxidation**	
PNGR/IPGR (in-vivo)	↓	↑	FAS	↓	PGC-1α	↑
			HMGCR	↓	CPT-1α	↑
Serum Starvation (in-vitro)	↓	↑	FAS	↑	PGC-1α	↑
			HMGCR	↑	CPT-1α	↑
Inhibitor (in-vitro)	↓	↑	FAS	↓	PGC1α	↓
			HMGCR	↓	CPT-1α	NC
MIMIC (in-vitro)	↑	↓	FAS	↑	PGC-1α	↑
			HMGCR	↑	CPT-1α	↑

↑ = increase, ↓ = decrease and NC = no change.